Physicochem. Probl. Miner. Process., 62(3), 2026, 224364

http://www.journalssystem.com/ppmp

Physicochemical Problems of Mineral Processing

ISSN 1643-1049

Simulation test on the blockage mechanism of fine suspended particles in ground leaching uranium

Wenjie Xiang, Qingliang Wang, Chunze Zhou

School of Resources, Environment and Safety Engineering, University of South China, Hengyang 421001, China

Corresponding author: zhouchunze89@126.com (Chunze Zhou)

Abstract: The "cliff-like" clogging in underground leaching uranium injection systems remains a critical technical challenge constraining production efficiency. Field observations indicate that fine suspended particles formed under acidic leaching conditions are the primary causative factors. This study systematically investigated the pressure variations and effluent turbidity patterns of silica fine suspended particles under different conditions (particle sizes: 1, 5, 30 μm; concentrations: 200-800 mg/L; filter mesh sizes: 50-400 mesh; solution flow rates: 30-120 mL/min), as well as the migration and clogging mechanisms of silica particles. Experimental results demonstrated that when silica particle sizes exceed filter mesh openings, rapid formation of filter cakes on the surface causes abrupt pressure surges. When particle sizes approach or fall below mesh dimensions, particles gradually deposit in internal pores, leading to deep-seated clogging. While larger filter mesh sizes effectively intercept fine particles, they significantly accelerate clogging progression. Although increased flow rates temporarily delay surface clogging, they elevate the risk of particle migration into deeper ore layers. This study reveals the multi-mechanism coupling characteristics of silica particle clogging in underground leaching processes, providing theoretical and experimental foundations for optimizing injection parameters.

Keywords: ground leaching uranium mining, silica fine suspended particles, clogging, filter screen

1. Introduction

As a third-generation uranium extraction technology, leaching has become the mainstream method for developing sandstone-type uranium resources globally due to its cost-effectiveness, high efficiency, and minimal environmental impact (Cai et al., 2015; Ingham and Pop, 1998; Li and Yao, 2024). This technique involves injecting specially formulated leaching solutions into ore layers to selectively dissolve uranium minerals under natural burial conditions, followed by recovery of the uranium-rich solution through a liquid extraction system (Su and Du, 2012; Liu et al., 2024; Li et al., 2024; Zhou et al., 2023a). However, in practical production, the continuous decline in injection capacity − particularly the "cliff-like" sudden blockages at wellbore filters − has led to increased well washing frequency and reduced effective working hours. These issues now represent a major technical bottleneck hindering the stable and efficient operation of leaching mines (Zhou et al., 2023b; Su and Du, 2019; Wang et al., 2015).

Field monitoring studies revealed that a certain acid leaching mine experienced a regular sharp decline in injection flow rate during the resin dilution transfer process (Zhang, 2005; Iler, 1979; Zho et al., 2001; Fang, 2023). Systematic analysis of the adsorption tailings and borehole sediments showed abnormally high SiO_2 concentrations, with the adsorption tailings containing 768 mg/L of SiO_2 and the white suspended matter in boreholes reaching 1.58 g/L (Hu et al., 2021; Scott et al., 2024; Guo et al., 2024). In acidic leaching environments, dissolved silicic acid (H_4SiO_4) undergoes polymerization as its concentration accumulates, gradually forming silicic acid sols and even gel-like polymers. These silicic acid polymers exhibit strong adsorption and cementation capabilities, readily depositing on filter mesh surfaces and internal pores. They are the primary causative substances leading to filter clogging and a sharp decline in liquid injection flow rates (Mew and Wyche, 2018; Kaneda et al., 2024).

DOI: 10.37190/ppmp/224364

Current research predominantly focuses on blockage mechanisms caused by chemical scaling (e.g., calcite and gypsum) or microbial metabolism in deep strata. Studies on solid particle-induced blockage in injection fluids mainly examine particle migration patterns within strata pores. However, systematic quantitative experimental investigations remain insufficient regarding the blockage characteristics, evolution patterns, and multi-parameter coupling effects of silica micro-suspensions at the wellbore filter–this critical bottleneck in the injection system. Compared with previous studies, the innovations of this study are summarized as follows: (1) The coupled effects of four key parameters, namely particle size, filter mesh number, flow velocity and solution concentration, were systematically quantified; (2) The critical conditions for the transition of clogging mechanism from surface filter cake formation to deep bridging were clarified; (3) Engineering-oriented design suggestions for gradient filters were proposed and preliminarily verified. At present, conventional hole flushing is the main on-site plug removal measure for siliceous particle-induced clogging, while targeted prevention and control schemes formulated based on clogging mechanisms are rarely adopted, leading to low plug removal efficiency and high economic cost.

Accordingly, the objectives of this study are as follows: (1) An indoor physical simulation experimental system was established to accurately reproduce filter clogging behaviors during the solution injection process of in-situ leaching; (2) The influence laws of particle size, filter mesh number, solution concentration and injection flow velocity on silica particle clogging characteristics were quantitatively revealed; (3) The dominant clogging mechanisms and coupling characteristics of multiple clogging mechanisms were clarified. This study can provide reliable data support and theoretical guidance for the optimal design of filters, regulation of injection process parameters, and targeted clogging prevention of solution injection systems in in-situ leaching uranium mining.

2. Experimental materials and methods

2.1. Experimental materials and instruments

To scientifically simulate the migration and clogging behavior of silica particles in the in-situ leaching system for uranium extraction, this experiment systematically investigated four key parameters: particle size, concentration, flow rate, and filter mesh size. The parameter selection was determined based on the particle characteristics of the leachate/adsorption tailings from the Nanlinggou uranium deposit and the actual operating conditions of the in-situ leaching process, with the specific rationale as follows:

(1) Particle size selection (1, 5, 30 μm): Based on the particle size distribution characteristics of SiO_2 in the adsorption tailings and borehole sediments from the leaching site, 1 μm represents colloidal particles formed by dissolved silicic acid polymerization, 5 μm corresponds to the main medium-sized suspended particles in the leaching solution, and 30 μm simulates large aggregates formed by silicic acid polymerization. This size range covers over 99.8% of the fine suspended particle scales in the field leaching solution, effectively reflecting the migration and retention behaviors of siliceous particles of different sizes in actual production.

(2) Concentration range (200-800 mg/L): Based on the SiO_2 concentration in the acid leaching tailings (768 mg/L) and the sediment SiO_2 content in boreholes (1.58 g/L), a 200-800 mg/L concentration gradient was established to simulate SiO_2 concentration fluctuations during the reuse of leaching and adsorption tailings in actual production processes, and to investigate the sensitivity of concentration to plugging kinetics (Meng et al., 2024).

(3) Flow rate range (30–120 mL/min): Based on the actual injection rate of the ground-infiltration solution well (typically 30–150 mL/min), four flow rate levels (30, 60, 80, and 120 mL/min) were established to investigate the dual effects of flow rate on particle transport and deposition behavior, including shear force, particle residence time, and convection-diffusion equilibrium.

(4) Mesh size (50–400 mesh): Five standard nylon filter meshes were selected (50 mesh: 279 μm, 150 mesh: 105 μm, 200 mesh: 76 μm, 300 mesh: 48 μm, 400 mesh: 38 μm) to cover the filtration precision of both the commonly used 50 mesh bag filter and the high-precision test filter. This was done to systematically investigate the impact of the ratio between filter mesh size and particle size on the clogging mechanism.

The porous medium was prepared using high-purity quartz sand (supplied by Tianjin Kemio Chemical Reagents Co., Ltd.), with SiO_2 content exceeding 99.0%, hydrochloric acid-soluble matter

below 0.2%, chloride content under 0.005%, and iron content less than 0.002%. After sieving, the quartz sand exhibited a porosity of 38%-42%, matching the porosity of sandstone-type uranium ore strata, effectively simulating the porous medium characteristics of the ore layer. The suspended particles used in the experiment were single-sized SiO_2 powders (supplied by Wuxi Taipeng Metal Materials Co., Ltd.), with a sphericity ≥0.9 and no surface-active groups, preventing chemical reactions between the suspended particles and the porous quartz sand. Three characteristic particle sizes (1 μm, 5 μm, and 30 μm) were selected to simulate fine particles released from the strata and micro-particles formed by silicic acid polymerization (Zhou, 2023).Although SiO_2 particles in practical systems exhibit complex morphologies including polydispersity, irregular shapes and gel state, monodisperse spherical particles were adopted in this study to eliminate the interference of chemical interactions and focus on physical clogging mechanisms.

The experimental filter screen is made of food-grade nylon 66 standard filter screen, the mesh size specifications include 50 mesh, 150 mesh, 200 mesh, 300 mesh and 400 mesh, the corresponding nominal aperture are 279 μm, 105 μm, 76 μm, 48 μm and 38 μm respectively, the thickness of the filter screen is 0.15 mm, the permeability rate is 80-120L/(m^2· s), so as to simulate the drilling filter of different precision grade in the field application.It should be noted that there are differences in flow convergence patterns between laboratory flat filters and field wrapped wire screens. Therefore, the research findings should be cautiously extended to practical engineering structures.

The core experimental setup is an independently designed "Borehole Simulation Column System". Constructed from PVC tubing, the column features a height of 800mm and an inner diameter of 200mm. It incorporates a dual-layer nylon mesh filter structure with an effective water pass-through area of 23%, containing 90 uniformly spaced holes spaced 10mm apart. The filter's flow characteristics match those of field injection borehole filters. Three pressure measurement holes are vertically distributed along the column's sidewall at 200mm intervals, each connected to a high-precision pressure sensor (measuring accuracy ±0.01kPa, range 0-200kPa).

The auxiliary experimental equipment includes: a BT100-1J peristaltic pump (controlling injection flow rate with precision of ±1%), a JJ-1 electric stirrer (operating at 0-3000 r/min to maintain suspension uniformity), a WGZ-200 turbidimeter (measuring inlet/outlet turbidity within 0-1000 NTU with ±0.1 NTU accuracy), and an Agilent 34970A data acquisition system (real-time pressure recording at 1Hz sampling frequency).All experiments were conducted at room temperature of 22±2°C. Given that the actual field temperature generally ranges from 40 to 60°C, the effects of temperature on silica gel polymerization and fluid viscosity were not simulated in this study. Temperature-controlled experiments are suggested for future investigations.

2.2. Experimental setup and procedures

The experimental setup primarily consists of a sand bucket, an experimental column, a pressure sensor, a peristaltic pump, a liquid extraction bucket, and a liquid collection bucket. The experimental column is equipped with two layers of nylon mesh filters to simulate the actual structure of an injection well, as shown in Fig. 1.

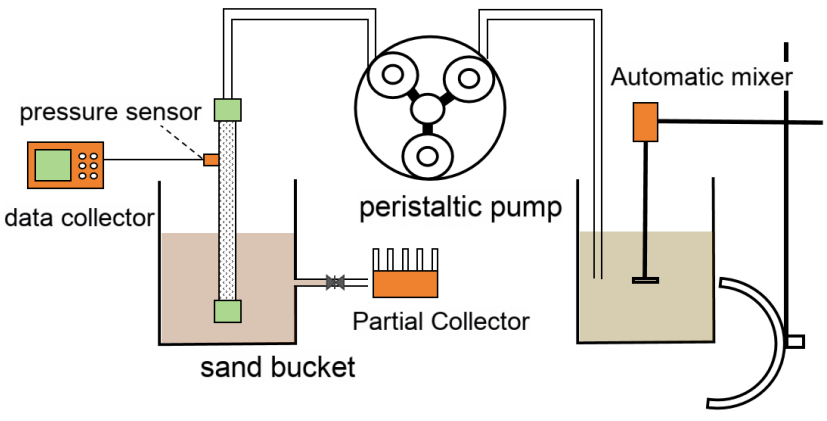

Fig. 1. Schematic diagram of the experimental apparatus

The experimental procedure is as follows:

(1) Quartz sand preparation: First, screen the quartz sand using a standard sieve to control particle size within the range of 0.18-0.42 mm (average 0.3 mm). To remove trace metal oxides and organic matter from the surface of the quartz sand, it is successively soaked in 0.1 M HCl solution and 0.1 M NaOH solution for 24 hours. After each soaking, the quartz sand is repeatedly washed with deionized water until neutral to remove surface impurities. The washed quartz sand is then dried in an oven at 105°C for 24 hours and stored after cooling.

(2) Pressure sensor installation: Install the pressure sensor at the pressure measurement hole of the test column, secure it with a butyl rubber water stop to ensure sealing, and connect it to the data acquisition system. Adjust the initial parameters of the data acquisition instrument, including range, unit, and sensor number, and perform zero calibration.

(3) Sample Loading and Saturation: Using a sample feeder, the pre-treated quartz sand is loaded into the column at 1 cm intervals. After each 1 cm increment, deionized water is added to maintain moisture, followed by gentle column wall tapping to expel air until the sand fills the column to the top. Subsequently, deionized water is slowly introduced from the bottom upward until water flows out of the column top without bubbles, ensuring complete saturation of the porous media. The column is then left undisturbed for 24 hours prior to use.

(4) Suspension preparation: Weigh specific particle size SiO_2 powder at required concentration using a 1:10,000 high-precision electronic balance, add corresponding volume of deionized water, and simultaneously activate the electric stirrer (800 r/min) for 30 minutes to ensure uniform dispersion and formation of suspension, preventing particle agglomeration.

(5) Suspension Permeation Test: After ensuring the seal integrity of the experimental column, a uniformly stirred suspension of specified concentration is pumped upward through a peristaltic pump into the sand column, aligning with the flow direction of the on-site injection well. The peristaltic pump controls the flow rate and volume of the suspension into the sand column, while the data acquisition instrument is activated to collect pressure readings from the pressure sensor at 1-minute intervals. When the peristaltic pump operates at low speed, suspended particles tend to adhere to the silica gel tube. To maintain stable particle concentration at the inlet, the silica gel tube should be kept straight and tilted vertically. Typically, the experiment continues for 24 hours after noticeable blockage occurs (as indicated by sudden pressure fluctuations or gradual stabilization), ensuring the blockage reaches a steady state before termination.

(6) Turbidity measurement: During the experiment, an automatic sampler was used to collect water samples from the inlet and outlet at 24-hour intervals, with each sample volume being 50 mL. The turbidity of the water samples was measured using a turbidimeter. Each group of water samples was measured three times in parallel, and the average value was taken. The difference in turbidity between the inlet and outlet (ΔNTU) was used to characterize the particle retention effect.

(7) Dimensionless number analysis: To verify the dynamic similarity between laboratory experiments and field conditions, characteristic parameters were calculated, including pore velocity ranging from 0.0016 to 0.0064 cm/s, Reynolds number (Re<0.1, satisfying Darcy flow regime), Peclet number (Pe=10–100, indicating particle migration dominated by convection), and Damköhler number (Da=0.01–0.1, suggesting a relatively low particle deposition rate which is favorable for investigating clogging evolution). These parameters are consistent with the typical in-situ conditions of sandstone-type uranium ore formations.

Particle mass balance analysis: to verify the reliability of the experimental data, particle mass balance was calculated based on the inlet concentration, outlet concentration, cumulative flow volume, and the mass of silica particles deposited on the filter screen and within the porous medium after each test. The mass balance recovery rate was determined using the following equation:

$$Recoveryrate(\%) = \frac{M_{out}+M_{deposited}}{M_{in}} \times 100\% \quad (1)$$

where M_{in} is the total injected particle mass, M_{out} is the total mass of particles in the effluent, and $M_{deposited}$ is the particle mass retained in the filter and porous medium. The recovery rates of all tests ranged from 92.3% to 97.6%, indicating good particle closure and high reliability of the experimental results.

2.3. Experimental design

This study designed nine experimental groups, systematically varying four key parameters: particle size, mesh size of the filter, concentration of fine silica particles, and injection flow rate. The experimental matrix is detailed in Table 1.

Table 1 Experimental Design Matrix

Experiment ID	mesh size of filter	normal pore size /μm	Particle size/μm	Silica concentration/(mg/L)	Inlet flow rate/(mL/min)	Experimental characteristics
1	200	76	30	200	30→80	Variable flow rate, large particle size
2	200	76	1	500	30	Constant flow rate, ultrafine colloidal particles
3	200	76	5	500	60/30 (day/night)	Variable flow rate, medium particle size
4	300	48	5	200	30	Constant flow rate, high-precision filter
5	300	48	30	200	30	Constant flow rate, particle size close to filter mesh aperture
6	400	38	1	400→800	80	Variable concentration, ultrafine colloidal particles + high-precision filter
7	400	38	30	400	80	constant concentration, large particle size + high-precision filter
8	400	38	5	400	60	constant concentration, medium particle size particles + high-precision filter
9	50	279	5	800	120	Constant concentration, on-site conventional filter screen + high flow rate

3. Results and discussion

3.1. Influence of particle size and mesh size on blockage and types of fine suspended particles

The relative size relationship between particle diameter (Dp) and filter calibration aperture (Df) is the primary controlling factor determining the initial clogging type and development rate. The pressure evolution characteristics of particles with different diameters are compared in Fig. 2.

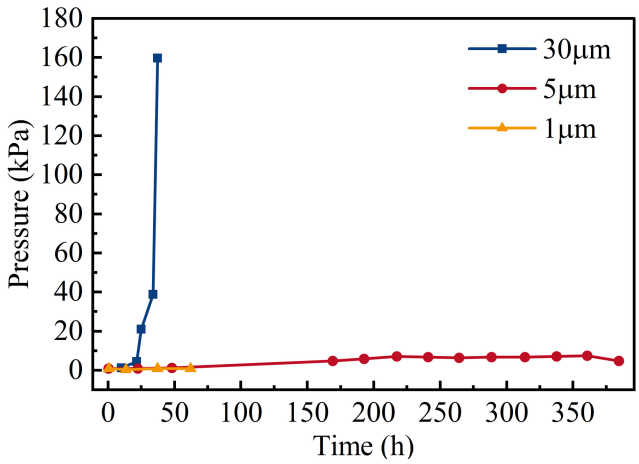

Fig. 2. Evolution of system pressure over time for SiO_2 particles of different sizes under a 200-mesh filter

According to the DLVO theory, particle deposition on media surfaces is governed by both van der Waals attraction and double-layer repulsion. The nylon filter used in this experiment carries a weak

negative charge, while SiO_2 particles also exhibit negative charge under acidic conditions, creating electrostatic repulsion between them. For 1 μm particles, their pronounced Brownian motion and relatively wide repulsion range make stable deposition difficult, allowing them to penetrate deeper layers. In contrast, 5 μm particles demonstrate reduced Brownian motion and enhanced van der Waals attraction. When their size approaches the filter pore diameter, they tend to form bridging effects at pore throat regions, creating initial deposition cores that trap more fine particles and accelerate deep-layer clogging.

Experiment 1 (200-mesh filter screen, $D_f \approx 76$ μm; 30 μm particles) demonstrated that particles approaching but smaller than the filter aperture were rapidly retained on the surface, forming a dense filter cake layer. Notably, after increasing the flow rate from 30 mL/min to 80 mL/min at 22 hours, the system pressure exhibited a "cliff-like" increase, surging from 4.54 kPa to 160.7 kPa within the subsequent 17 hours−a pressure rise exceeding 40-fold. Post-experiment dissection (Fig. 3) revealed a 2-3 mm thick white SiO_2 deposit layer covering the filter surface, confirming the dominant role of surface filter cake clogging mechanisms.

Fig. 3. Post-experiment dissection

Experiment 2 (200-mesh filter; 1 μm particles) exhibited markedly different behavioral characteristics. As the particle size was significantly smaller than the filter aperture ($D_p << D_f$), the system pressure remained stable throughout the 264-hour experiment (fluctuating within 1.0-1.2kPa), with the inlet-outlet turbidity difference consistently maintained at a low level (ΔNTU<5). This indicates that most small-sized particles penetrated the filter and entered the simulated formation zone. Although this did not cause significant clogging of the filter itself, it created a latent risk of long-term blockage in the deep pore system of the formation.

Experiments 3 (200-mesh filter; 5 μm particles) and 5 (300-mesh filter, $D_f \approx 50$ μm; 30 μm particles) demonstrated more complex deep-sea blockage behaviors. When the particle-to-filter aperture ratio approached the critical bridging condition ($D_p \approx D_f$), particles were partially retained on the filter surface while others entered the internal pore structure, forming gradual yet persistent deep-sea blockage through bridging and deposition. Monitoring data from Experiment 5 showed that system pressure began to rise significantly on day 4, followed by a steady upward trend, while filtrate turbidity started declining from day 7 and eventually reached an extremely low level of 1.33 NTU. Although filtration efficiency remained exceptionally high at this stage, the effective flow area had drastically decreased, with the feed flow rate dropping to less than 10% of the initial value. Fig. 4, an anatomical photograph, clearly illustrates the state of the filter's internal pores being filled with abundant SiO_2 particles.

The experimental results are in good agreement with the classical particle clogging theory model (Zhang et al., 2024). Herzig et al. (1970) proposed the bridging theory, which indicates that the transition

from 'cake filtration' to 'deep filtration' in clogging behavior primarily depends on the critical ratio of D_p/D_f.When the local infiltration system injects silica particles with a broad particle size distribution into the liquid, it simultaneously triggers two clogging mechanisms: surface filter cake formation and deep bridging deposition, significantly increasing the difficulty and complexity of prevention and control (Me et al., 2020).The particle mass balance was verified for all experiments, with recovery rates between 92.3% and 97.6%, confirming the accuracy of the pressure and turbidity measurements.

Fig. 4. Anatomical photograph

3.2. Effect of injection flow rate on particle clogging and retention behavior

The influent flow rate significantly influences the deposition location and clogging development pattern of particles in the filter by altering fluid shear force and particle transport dynamics. The effect of flow rate is illustrated in Fig. 5.

The effect of flow velocity on particle deposition can be understood through the Peletier number (Pe) and Schmidt number (Sc). The Pe number characterizes the relative importance of convective transport

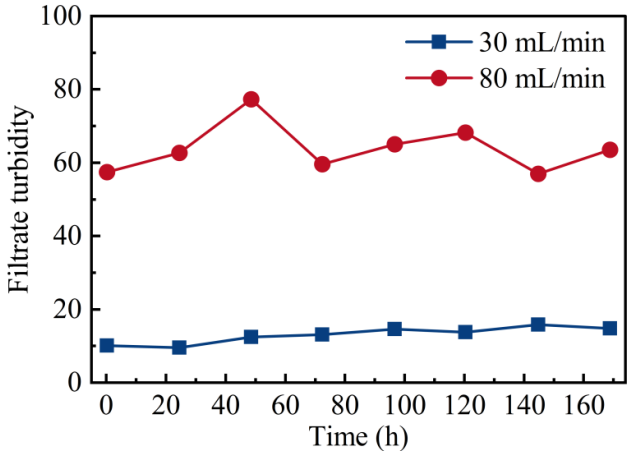

Fig. 5. Evolution of filtrate turbidity of 1 μm SiO_2 particles under 400-mesh filter

versus diffusive transport, while the Sc number reflects the relative rates of momentum diffusion and mass diffusion (Mardanov et al., 2023).

At high flow rates (increased Pe number), convection dominates, causing particles to penetrate the filter screen with the fluid, resulting in increased turbidity. At low flow rates (decreased Pe number), diffusion becomes more pronounced, allowing particles more time to deposit on the filter surface and promoting filter cake formation. Meanwhile, a high Sc number (common in colloidal systems) indicates slower particle diffusion. Increased flow velocity further inhibits diffusion deposition, which aligns with the experimental observation that "high flow rates delay surface clogging but increase the risk of deep migration."

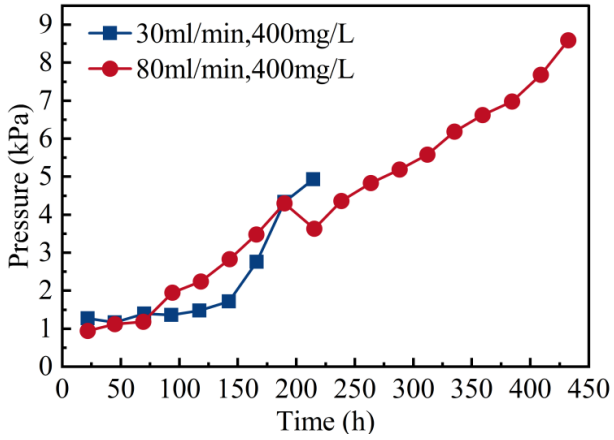

Fig. 6. Effects of flow velocity variation on pressure characteristics

Comparative analysis of pressure development data from Experiment 1 (initial flow rate of 30 mL/min) and Experiment 7 (80 mL/min) revealed that under identical particle size (30 μm) and similar filter screen precision conditions, the pressure increase rate at lower flow rates was significantly faster than at higher flow rates. Specifically, in Experiment 1 at 30 mL/min flow rate, the pressure reached 4.54 kPa within the first 22 hours, whereas in Experiment 7 at 80 mL/min flow rate, the pressure only increased to 1.45 kPa during the same period. This indicates that lower flow rates provide more time for particle deposition and aggregation on the filter screen surface, thereby accelerating the formation and development of the filter cake.

The turbidity comparison between Experiment 6 (400-mesh filter, 1 μm particles, 80mL/min) and Experiment 5 (300-mesh filter, 1 μm particles, 30mL/min) further reveals the complex effects of flow velocity. Throughout the experiment, the filtrate turbidity in Experiment 6 remained consistently high (50-77 NTU), while in Experiment 5, it was only 10-15 NTU during comparable phases. This phenomenon suggests that the intense fluid dynamics generated by high flow velocity may "wash" through the filter screen the fine particles that should be retained, or prevent their stable deposition on the filter surface, leading to elevated turbidity. However, this apparent "improvement" actually implies that more particles penetrate deeper into the formation, potentially causing more challenging deep-seated formation blockages.

In their study on colloidal particle migration in porous media, Bradford and Torkzaban (2008) demonstrated that flow velocity exerts a dual effect on particle deposition: while increased flow velocity reduces particle residence time on the medium surface and consequently decreases deposition probability, it simultaneously enhances convective mass transfer to the surface, potentially increasing deposition under specific conditions. The observed phenomena in this research corroborate this theoretical understanding, confirming that flow velocity in ground leaching systems functions as a "double-edged sword" requiring careful regulation to balance the dual risks of surface filter clogging and deep-layer formation blockage.

3.3. Effects of solution concentration and mesh size on filtration performance

The solution concentration directly affects the particle flux reaching the filter surface per unit time, serving as a critical parameter for controlling clogging progression. The mesh size determines the filter's

retention accuracy and initial flow resistance, acting as the core factor influencing clogging patterns and development rates. Fig. 6 illustrates the pressure evolution patterns of 5 μm SiO_2 particles under varying mesh sizes and concentrations.

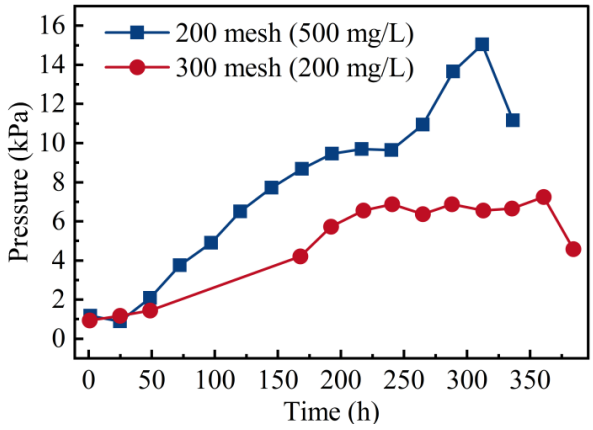

Fig. 7. Evolution of system pressure over time for 5 μm SiO_2 particles at different mesh sizes

The monitoring data from Experiment 6 revealed that as the concentration of 1 μm particles increased from 400 mg/L to 800 mg/L, the system pressure rose significantly from approximately 1.5 kPa to around 5 kPa. This demonstrates that higher particle load indeed results in faster deposition rates. The observed phenomenon aligns with the classical particle deposition kinetics theory, which posits a direct correlation between deposition rate and particle concentration.

However, a comparative analysis of Experiment 3 (200-mesh filter, 500 mg/L, 5 μm particles) and Experiment 4 (300-mesh filter, 200 mg/L, 5 μm particles) revealed more profound patterns. Although the particle concentration in Experiment 4 was only 40% of that in Experiment 3, its final steady pressure (15.08 kPa) was significantly higher than that in Experiment 3 (7.28 kPa). Post-experiment anatomical observations also demonstrated markedly more severe clogging in Experiment 4. This comparison strongly indicates that under these experimental conditions, the influence of filter precision on clogging development far outweighs the effect of solution concentration.

3.4. Conceptual model of plugging evolution under multi-mechanism coupling

Based on the experimental results and theoretical analysis, we propose a multi-mechanism coupled evolution conceptual model for the blockage of silica particles in the ground infiltration system.

Initial stage: The injected fluid carries a multiparticle swarm that reaches the filter surface. Larger particles ($D_p > D_f$) are directly retained on the filter surface, initiating the formation of filter cake. Medium-sized particles ($D_p \approx D_f$) undergo bridging effects at pore throat channels, causing initial internal pore blockage. Smaller particles ($D_p << D_f$) predominantly pass through the filter and enter deeper strata.

Development Stage: The surface filter cake progressively thickens, with flow resistance exhibiting exponential growth. Deep bridging particles act as "collection cores," continuously capturing subsequent fine particles, leading to a significant decrease in internal porosity. Particles entering the formation zone gradually deposit in the low-velocity zone, initiating the formation of secondary plugging layers. Different plugging mechanisms exhibit synergistic enhancement effects.

Stabilization/Uncontrolled Phase: The surface filter cake becomes compact or internal pores are fully filled, with system pressure drop reaching engineering limits and injection flow rate dropping below economic recovery levels. At this stage, the system enters either a stable clogging state or complete uncontrolled state, requiring clogging removal measures to resume production.

This conceptual model can explain the phenomenon of "cliff-like" blockage observed in the field, that is, when the system develops to a certain critical state, the various blockage mechanisms are coupled with each other, resulting in a sharp deterioration of the injection capacity in a short time.

Filtration coefficient fitting: The experimental data were fitted to the deep bed filtration model proposed by Herzig et al. The filtration coefficient λ was fitted via the formula: $\ln(C/C_0)=-\lambda L$, where C and C_0 represent the outlet and inlet concentrations, respectively, and L denotes the thickness of the filter layer. The fitting results reveal that the filtration coefficient λ increases with the rise of filter mesh number and particle size, which is consistent with the variation trend of the classical model and verifies the reliability of the experimental data obtained in this study.

4. Conclusions and recommendations

4.1. Conclusions

(1) The blockage of the leaching system by silica particles is the result of the interaction between the surface filter cake and the deep bridging, and the dominant mechanism is determined by the relative size of the particle size and the filter mesh aperture.
(2) The mesh size of the filter is the most sensitive factor affecting the rate and extent of clogging. Although high-precision filters exhibit excellent retention efficiency, they significantly shorten the injection cycle.
(3) Flow velocity has a dual effect: low flow velocity accelerates surface clogging of the filter screen, while high flow velocity may delay surface clogging but increases the risk of deep formation clogging.
(4) The influence of solution concentration on the development of clogging is relatively weak. Within the experimental concentration range (200-800 mg/L), the effect of concentration variation on clogging velocity is significantly less than that of filter mesh size.

4.2. Recommendations

Based on the main conclusions of this study, the following engineering suggestions are proposed for the clogging prevention and control of the solution injection system in in-situ leaching uranium mining:

(1) Optimize the structural design of filter screens. Gradient or composite filter screen structures are recommended, with multi-stage filters featuring progressively increasing mesh numbers arranged from the outside to the inside. Preliminary experimental results verify that gradient filters can extend the clogging duration by approximately 40% compared with single-layer 400-mesh filters. This design enables pre-filtration of coarse particles and final interception of fine particles, which effectively prolongs the service life of filters while guaranteeing the quality of injected solution.
(2) Adopt intelligent solution injection strategies. Pulsed injection or variable flow-rate injection technologies are suggested to be developed. Periodic high-flow-rate flushing can erode initially formed filter cakes and inhibit their continuous growth. In addition, intelligent flow rate regulation can balance the risks of surface clogging and deep-layer clogging.
(3) Strengthen pre-treatment procedures. Prior to solution injection, solid-liquid separation treatments including gravitational sedimentation and medium filtration should be conducted for lixiviant or recycled tail liquid to reduce the particle concentration of injected fluid at the source.
(4) Establish an early warning and monitoring system. Early warning indicators for clogging of the injection system are established according to the rising rate of system pressure and variation characteristics of filtrate turbidity.
(5) Prospective research directions. Temperature-controlled experiments are recommended to clarify the effects of actual formation temperature (40–60°C) on silica gel polymerization and system clogging. Non-spherical and gelatinous SiO_2 particles, actual ore samples and clay mineral-containing porous media are suggested to be applied in subsequent tests. Furthermore, pilot-scale tests should be performed to verify the practical effectiveness of gradient filter screens and pulsed solution injection technologies.

Acknowledgments

We thank the following funding agencies for supporting this work: Excellent Young Scientist Project of Scientific Research Fund of Hunan Provincial Education Department, China (Grant No. 24B0381).

References

BRADFORD S. A., TORKZABAN S., 2008. *Colloid transport and retention in unsaturated porous media: A review of interface-, collector-, and pore-scale processes and models*. Vadose Zone Journal, 7(2), 667–681.

CAI Y. Q., ZHANG J. D., LI Z. Y. i in., 2015. *Summary of characteristics and mineralization laws of uranium resources in China*. Acta Geologica Sinica, 89(06), 1051–1069.

FANG M. T., 2023. *Study on the Reaction Kinetics of Calcium Carbonate Minerals and the Influence of Blockage in Acidic Leaching for Uranium Extraction*. Fuzhou, Donghua University of Science and Technology (D).

GUO J., ZHOU Z., GE Y. i in., 2024. *High flow-rate pre-leaching of low-grade uranium ore: gypsum reduction*. Journal of Radioanalytical and Nuclear Chemistry, 333(4), 2183–2193.

HERZIG J. P., LECLERC D. M., GOFF P. L., 1970. *Flow of suspensions through porous media—application to deep filtration*. Industrial & Engineering Chemistry, 62(5), 8–35.

HU P. F., XING Y. G., LIU J. H., 2021. *Migration of silicon and its impact on production systems in an acid leaching uranium mine*. Nonferrous Metals (Smelting Section), (08), 56–64.

ILER R. K., 1979. *The Chemistry of Silica: Solubility, Polymerization, Colloid and Surface Properties, and Biochemistry*. New York, Wiley.

INGHAM D. B., POP I., 1998. *Transport Phenomena in Porous Media*. Oxford, Elsevier.

KANEDA M., CAO T., DONG D. i in., 2024. *Inhibition of silica scaling with functional polymers: Role of ionic strength, divalent ions, and temperature*. Water Research, 258, 121705.

LI G., YAO J., 2024. *A review of in situ leaching (ISL) for uranium mining*. Mining, 4(1), 120–148.

LI J., FENG J., XUE J. i in., 2024. *The influence of surfactants on the acid leaching process of a uranium mine in Inner Mongolia*. Journal of Radioanalytical and Nuclear Chemistry, 333(11), 5845–5855.

LIU Y., HE Y., CHEN J. i in., 2024. *Progress on enhancing seepage-leaching mass-transfer research for in-situ leaching mining of low-permeability uranium-bearing sandstone: A review*. Journal of Radioanalytical and Nuclear Chemistry, 333(9), 4485–4502.

MA T., PENG N., CHEN P., 2020. *Filter cake formation process by involving the influence of solid particle size distribution in drilling fluids*. Journal of Natural Gas Science and Engineering, 79, 103350.

MARDANOV R., ZARIPOV S., SHARAFUTDINOV V., 2023. *The theoretical study of the efficiency of diffusion deposition of nanoaerosols in the extended range of the Peclet numbers*. Particuology, 77, 47–55.

MENG Q., SHI F., FAN W. i in., 2024. *SiO_2 and microparticle transport in a saturated porous medium: effects of particle size and flow rate*. Applied Water Science, 14(3), 50.

MEW M., WYCHE N., 2018. *The geochemical challenges of in-situ recovery mining*. Applied Geochemistry, 97, 121–132.

SCOTT S., GALECZKA I. M., GUNNARSSON I. i in., 2024. *Silica polymerization and nanocolloid nucleation and growth kinetics in aqueous solutions*. Geochimica et Cosmochimica Acta, 371, 78–94.

SU X. B., DU Z. M., 2012. *Development status and prospects of underground leaching technology for uranium extraction in China*. China Mining, 21(09), 79–83.

SU X. B., DU Z. M., 2019. *Research progress on the mechanism and prevention technology of borehole plugging in underground uranium mining*. Uranium Mining and Metallurgy, 38(3), 157–162.

WANG L. M., LIAO W. S., XU Y. i in., 2015. *Study and evaluation of permeability damage caused by micro-particle migration in sandstone uranium ore beds*. Uranium Mining and Metallurgy, 34(04), 235–240, 244.

ZHANG S., ZENG Z., YUAN H. i in., 2024. *Precursory arch-like structures explain the clogging probability in a granular hopper flow*. Communications Physics, 7(1), 202.

ZHANG Z. G., 2005. *Exploratory study on chemical descaling for blockage of underground uranium ore deposits*. Uranium Mining and Metallurgy, (04), 14–18.

ZHOU C., 2023. *Physical blockage mechanism and control of suspended particles in groundwater leaching uranium*. Hengyang, Nanhua University (D).

ZHOU C. Z., WANG H. Q., WU T. P., HU E. M., LEI Z. W., WANG Q. L., 2023a. *Simulation study on clogging of suspended particles in in-situ leaching of uranium at different concentrations and flow velocity*. Physicochemical Problems of Mineral Processing, 59(2).

ZHOU C. Z., WANG H. Q., WU T. P., HU E. M., LEI Z. W., WANG Q. L., 2023b. *Study on the clogging of suspended particles with different particle sizes in porous media in in situ leaching of uranium*. Journal of Radioanalytical and Nuclear Chemistry, 332(10), 4243–4253.

ZHOU Y. M., SHEN Z. L., SUN Z. X., 2001. *Review on the dissolution and precipitation of silica in water-rock interactions*. Geoscientific Frontiers, 8(4), 415–422.